Dynamics of Solitary-waves in the Higher Order Korteweg – De Vries Equation Type (I)

Woo-Pyo Hong

Department of Photonics and Information Engineering, Catholic University of Daegu, Hayang, Kyongsan, Kyungbuk 712-702, South Korea

Reprint requests to Prof. W.-P. H.; E-mail: wphong@cu.ac.kr

Z. Naturforsch. **60a,** 757 – 767 (2005); received June 30, 2005

We find new analytic solitary-wave solutions of the higher order wave equations of Korteweg – De Vries (KdV) type (I), using the auxiliary function method. We study the dynamical properties of the solitary-waves by numerical simulations. It is shown that the solitary-waves are stable for wide ranges of the model coefficients. We study the dynamics of the two solitary-waves by using the analytic solution as initial profiles and find that they interact elastically in the sense that the mass and energy of the system are conserved. This leads to the possibility of multi-soliton solutions of the higher order KdV type (I), which can not be found by current analytical methods. – PACS numbers: 03.40.Kf, 02.30.Jr, 47.20.Ky, 52.35.Mw

Key words: Generalized Korteweg – De Vries Equation Type (I); Analytic Solitary-wave Solutions; Numerical Simulation; Stability; Interaction Dynamics.

1. Introduction

In this paper we consider higher order wave equations of the Korteweg – De Vries (KdV) type (I)

$$v_t + v_x + \alpha v v_x + \beta v_{xxx} + \alpha^2 \rho_1 v^2 v_x + \alpha\beta\rho_2 v v_{xxx} + \alpha\beta\rho_3 v_x v_{xx} = 0, \quad (1)$$

where ρ_i $(i = 1, 2, 3)$ are free parameters and α, β are real constants characterizing, respectively, the long wavelength and short amplitude of the waves [1 – 5]. This equation describes unidirectional wave motion on the surface of a thin layer of an inviscid and incompressible fluid, and $v(x,t)$ represents the normalized dimensionless amplitude of the fluid surface with respect to its level at rest compared with the depth of the layer [4, 5]. We note that in the following analysis of (1) the spatial and time variables x and t, and the model coefficients are normalized to be dimensionless [2, 3]. This equation is valid for $\alpha, \beta \ll 1$, obeying $\beta < \alpha$, and in general is nonintegrable in the sense that some of its ordinary differential equation reductions do not possess the Painlevé property and can not find the Lax pairs [4, 5].

Some traveling sech^2-type solitary-wave solutions of (1) have been obtained, and their dynamical behavior has been numerically investigated in [4, 5]. Recently, Long et al. [6] have proved the existence of smooth solitary waves and infinitely many smooth and nonsmooth periodic wave solutions of (1) using the method of planar dynamics systems. More recently, Li and Liu [7, 8] have shown the existence of nonsmooth traveling wave equations. On the other hand, Jeffrey and Mohamad [9] presented a direct method for the construction of traveling wave solutions.

The purpose of this paper is to find new sech^4-type analytic traveling solitary-wave solutions of (1), by using the auxiliary differential equation method [10 – 12], which are different from the previously obtained ones, and investigate their dynamic behavior. In Section 2 we introduce the auxiliary differential equation method and perform symbolic computations. In Section 3 we investigate the dynamics of the solitary-waves using the numerical method. The conclusions are in Section 4.

2. The Auxiliary Equation Method and Analytic Solitary-wave Solution

In this section, we first describe the auxiliary equation method [10, 11]. Suppose we are giving a nonlinear partial differential equation (NLPDE) for $v(x,t)$ in the form

$$H(v, v_x, v_t, v_{xx}, v_{tt}, v_{xt} \ldots) = 0. \quad (2)$$

Introducing the similarity variable $\xi = kx - \omega t$, the traveling wave solution of $v(\xi)$ satisfies the ODE

$$G(v, v_\xi, v_{\xi\xi}, v_{\xi\xi\xi}, \ldots) = 0. \tag{3}$$

By virtue of the extended tanh-function method one assumes that the solution of (3) has the form

$$v(\xi) = \sum_{i=0}^{n} a_i z^i(\xi), \tag{4}$$

in which a_i ($i = 1, 2, \ldots, n$), k and ω are real constants to be determined, the order n is a positive integer which can be determined by balancing the highest order derivative term with the highest power nonlinear term in (3), and $z(\xi)$ expresses the solutions of the auxiliary ordinary differential equation

$$\left(\frac{\mathrm{d}z}{\mathrm{d}\xi}\right)^2 = az^2(\xi) + bz^3(\xi) + cz^4(\xi), \tag{5}$$

where a, b, and c are real parameters. We seek the exact solutions of (3) by using the solutions of (5)

$$z(\xi) = \begin{cases} \dfrac{-ab\,\mathrm{sech}^2(\pm\frac{\sqrt{a}}{2}\xi)}{b^2 - ac(1 - \tanh(\pm\frac{\sqrt{a}}{2}\xi))^2}, & \text{when } a > 0, \\ \dfrac{2a\,\mathrm{sech}(\sqrt{a}\xi)}{\sqrt{b^2 - 4ac} - b\,\mathrm{sech}(\sqrt{a}\xi)}, \\ \qquad \text{when } \sqrt{b^2 - 4ac} > 0 \text{ and } a > 0. \end{cases} \tag{6}$$

To look for the traveling wave solutions of (1), we make the transformation $v(x, t) = v(\xi)$, leading to

$$\begin{aligned} &(-\omega + \alpha k v + \alpha^2 \rho_1 k v^2 + k + \alpha\beta\rho_3 k^3 v_{\xi\xi}) v_\xi \\ &\quad + (\alpha\beta\rho_2 v k^3 + \beta k^3) v_{\xi\xi\xi} = 0. \end{aligned} \tag{7}$$

Balancing the highest order derivative $\alpha\beta\rho_2 k^3 v v_{\xi\xi\xi}$ with the highest power nonlinear term $\alpha^2\rho_1 k v^2 v_\xi$ in (7) yields to $n = 2$. Therefore, we choose a solution of (7) in the form

$$v(\xi) = a_0 + a_1 z(\xi) + a_2 z(\xi)^2, \tag{8}$$

where a_0, a_1, and a_2 are constants to be determined. By substituting (5) and (8) into (7) and setting the coefficients of $z^j(\xi)(j = 0, 1, 2, \ldots, 7)$ to zero, we find a set of algebraic equations for a, b, c, a_0, a_1, a_2, k, and ω:

$$\begin{aligned} &a_1\alpha^2\rho_1 k a {a_0}^2 + a_1(\alpha k + a\rho_2\alpha k^3\beta) a a_0 \\ &+ a_1(-\omega + k + ak^3\beta) a = 0, \end{aligned} \tag{9}$$

$$\begin{aligned} &(b{a_1}\alpha^2\rho_1 k + 2a a_2\alpha^2\rho_1 k){a_0}^2 \\ &+ (4b\beta k^3\alpha\rho_2 a_1 a + b{a_1}\alpha k + 8\beta k^3\alpha\rho_2 a_2 a^2 \\ &\quad + 2a\alpha^2 k {a_1}^2\rho_1 + 2a a_2\alpha k) a_0 - b{a_1}\omega \\ &+ 2a a_2 k + \alpha\beta\rho_2 {a_1}^2 k^3 a^2 + 4b\beta k^3 a_1 a \\ &- 2a a_2\omega + b{a_1}k + 8\beta k^3 a_2 a^2 \\ &+ {a_1}^2\alpha\beta\rho_3 k^3 a^2 + a\alpha k {a_1}^2 = 0, \end{aligned} \tag{10}$$

$$\begin{aligned} &(2b a_2\alpha^2\rho_1 k + c a_1\alpha^2\rho_1 k) a_0^2 \\ &+ (23b\beta k^3\alpha\rho_2 a_2 a + c a_1\alpha k + 2b\alpha^2 k a_1^2\rho_1 \\ &\quad + 7c\beta k^3\alpha\rho_2 a_1 a + 3\beta k^3\alpha\rho_2 a_1 b^2 \\ &\quad + 2b a_2\alpha k + 6a\alpha^2 k a_2\rho_1 a_1) a_0 \\ &+ 9\alpha\beta\rho_2 a_1 k^3 a_2 a^2 - 2b a_2\omega + 3a\alpha k a_2 a_1 \\ &+ \frac{5}{2} b a_1^2\alpha\beta\rho_3 k^3 a + 7c\beta k^3 a_1 a + 2b a_2 k \\ &+ a\alpha^2 k a_1^3\rho_1 + 3\beta k^3 a_1 b^2 + 23b\beta k^3 a_2 a \\ &- c a_1\omega + 4b\alpha\beta\rho_2 a_1^2 k^3 a + b\alpha k {a_1}^2 + c a_1 k \\ &+ 6a_1\alpha\beta\rho_3 k^3 a_2 a^2 = 0, \end{aligned} \tag{11}$$

$$\begin{aligned} &2c a_2\alpha^2\rho_1 {a_0}^2 k \\ &+ (2c a_2\alpha k + 6b\alpha^2 k a_2\rho_1 a_1 + 4a\alpha^2 {a_2}^2 k\rho_1 \\ &\quad + 15\beta k^3 a_2\alpha\rho_2 b^2 + 32c\beta k^3\alpha\rho_2 a_2 a \\ &\quad + 2c\alpha^2 k {a_1}^2\rho_1 + 9c\beta k^3\alpha\rho_2 a_1 b) a_0 \\ &+ 2c a_2 k - 2c a_2\omega + 14a_1\alpha\beta\rho_3 k^3 a_2 a b \\ &+ 8{a_2}^2\alpha\beta\rho_3 k^3 a^2 + 9c\beta k^3 a_1 b \\ &+ 4a\alpha^2 a_2 k\rho_1 {a_1}^2 + 7c\alpha\beta\rho_2 {a_1}^2 k^3 a \\ &+ 3c{a_1}^2\alpha\beta\rho_3 k^3 a + 2a\alpha {a_2}^2 k \\ &+ 32c\beta k^3 a_2 a + c\alpha k {a_1}^2 + 15\beta k^3 a_2 b^2 \\ &+ 3\alpha\beta\rho_2 {a_1}^2 k^3 b^2 + 27b\alpha\beta\rho_2 a_1 k^3 a_2 a \\ &+ 3b\alpha k a_2 a_1 + \frac{3}{2}{a_1}^2\alpha\beta\rho_3 k^3 b^2 \\ &+ b\alpha^2 k {a_1}^3\rho_1 + 8\alpha k^3\beta\rho_2 {a_2}^2 a^2 = 0, \end{aligned} \tag{12}$$

$$\begin{aligned} &\frac{1}{2}k(78k^2 c\beta a_2\alpha\rho_2 b + 12k^2\beta\alpha\rho_2 a_1 c^2 \\ &\quad + 12c\alpha^2 a_2\rho_1 a_1 + 8b\alpha^2 {a_2}^2\rho_1) a_0 \\ &+ \frac{1}{2}k(12k^2 c^2 a_1\beta + 7k^2 c{a_1}^2\alpha\beta\rho_3 b \\ &\quad + 78k^2 c\alpha\beta\rho_2 a_1 a_2 a + 78k^2 b a_2\beta c \\ &\quad + 18k^2 c\alpha\beta\rho_2 {a_1}^2 b + 16k^2 a_1\alpha\beta\rho_3 a_2 b^2 \\ &\quad + 46k^2 b\alpha\beta\rho_2 {a_2}^2 a + 36k^2\alpha\beta\rho_2 a_1 a_2 b^2 \\ &\quad + 32k^2 a_1\alpha\beta\rho_3 a_2 a c + 4b\alpha {a_2}^2 \\ &\quad + 2c\alpha^2 {a_1}^3\rho_1 + 36k^2 {a_2}^2\alpha\beta\rho_3 a b \\ &\quad + 8b\alpha^2 a_2\rho_1 {a_1}^2 + 10a\alpha^2\rho_1 a_1 {a_2}^2 \\ &\quad + 6c\alpha a_2 a_1) = 0, \end{aligned} \tag{13}$$

$$
\begin{aligned}
&k(24k^2\beta\alpha\rho_2 a_2 c^2 + 4c\alpha^2 {a_2}^2\rho_1)a_0 \\
&+ k(6k^2\alpha\beta\rho_2 {a_1}^2 c^2 + 10k^2 {a_2}^2\alpha\beta\rho_3 b^2 \\
&\quad + 24\beta a_2 c^2 k^2 + 18k^2 a_1\alpha\beta\rho_3 a_2 bc \\
&\quad + 48k^2 c\alpha\beta\rho_2 a_1 a_2 b + 32k^2 c\alpha\beta\rho_2 {a_2}^2 a \\
&\quad + 2k^2 {a_1}^2\alpha\beta\rho_3 c^2 + 2a\alpha^2\rho_1 {a_2}^3 \\
&\quad + 15k^2\alpha\beta\rho_2 {a_2}^2 b^2 + 20k^2 {a_2}^2\alpha\beta\rho_3 ac \\
&\quad + 4c\alpha^2 a_2\rho_1 {a_1}^2 + 2c\alpha {a_2}^2 \\
&\quad + 5b\alpha^2\rho_1 a_1 {a_2}^2) = 0,
\end{aligned} \tag{14}
$$

$$
\begin{aligned}
&\alpha k a_2(2\alpha b\rho_1 {a_2}^2 + 5\alpha c\rho_1 a_1 a_2 + 22k^2 a_2\beta\rho_3 bc \\
&\quad + 39k^2 a_2 c\beta\rho_2 b + 10k^2 a_1\beta\rho_3 c^2 \\
&\quad + 30k^2\beta\rho_2 a_1 c^2) = 0,
\end{aligned} \tag{15}
$$

$$
2\alpha ck {a_2}^2(\rho_1 a_2\alpha + 6ck^2\beta\rho_3 + 12ck^2\beta\rho_2) = 0. \tag{16}
$$

By solving these overdetermined algebraic equations, we obtain

$$
\begin{aligned}
a_0 &= \frac{(\mathcal{L}_1 k^2 - \frac{1}{2}c\rho_3 - c\rho_2 + c\rho_1)}{c\rho_1\alpha(\rho_3 + \rho_2)}, \\
a_1 &= -3\frac{k^2\beta b(\rho_3 + 2\rho_2)}{\alpha\rho_1}, \\
a_2 &= -6\frac{c\beta k^2(\rho_3 + 2\rho_2)}{\alpha\rho_1}, \\
\omega &= \frac{(\mathcal{L}_2 k^5 + \mathcal{L}_3 k)}{c^2\rho_1({\rho_3}^2 + 2\rho_3\rho_2 + {\rho_2}^2)},
\end{aligned} \tag{17}
$$

where

$$
\begin{aligned}
\mathcal{L}_1 &= \Big(\frac{3}{8}\beta b^2 {\rho_3}^2 + \frac{3}{4}\beta {\rho_2}^2 b^2 + \frac{9}{8}\beta b^2\rho_3\rho_2 \\
&\quad - 2c\beta {\rho_3}^2 a - 6c\beta\rho_3 a\rho_2 - 4\beta {\rho_2}^2 ca\Big), \\
\mathcal{L}_2 &= \Big(\frac{1}{16}\beta^2 b^4 {\rho_3}^3\rho_2 + \frac{1}{32}\beta^2 b^4\rho_3 {\rho_2}^3 \\
&\quad + \frac{1}{64}\beta^2 b^4 {\rho_3}^4 + \frac{5}{64}\beta^2 b^4 {\rho_3}^2 {\rho_2}^2\Big), \\
\mathcal{L}_3 &= \Big(c^2 {\rho_1}^2 - \frac{1}{2}c^2\rho_3\rho_2 + 2c^2\rho_1\rho_3\rho_2 + c^2\rho_1 {\rho_3}^2 \\
&\quad - c^2\rho_2\rho_1 - \frac{1}{4}c^2 {\rho_3}^2 + c^2\rho_1\rho_2^2\Big),
\end{aligned} \tag{18}
$$

under the constraint among a, b, and c

$$
b^2 - 4ac = 0. \tag{19}
$$

This condition in fact indicates that the solution set in (17) satisfies only the type (I) solution in (6) if, in conjunction with the constraint $a = b^2/4c > 0$, we require the parameters to satisfy $c > 0$. Upon substituting all this into (7), we find a new analytic solitary-wave solution of (1), where b, c, and k are free parameters of the form

$$
\begin{aligned}
v(x,t) = &\frac{\mathcal{L}_1 k^2 - \frac{1}{2}c\rho_3 - c\rho_2 + c\rho_1}{c\rho_1\alpha(\rho_3 + \rho_2)} \\
&- \frac{3k^2\beta b(\rho_3 + 2\rho_2)}{\alpha\rho_1}\Lambda(x,t) \\
&- \frac{6c\beta k^2(\rho_3 + 2\rho_2)}{\alpha\rho_1}\Lambda(x,t)^2,
\end{aligned} \tag{20}
$$

where

$$
\Lambda(x,t) = \frac{-ab\,\mathrm{sech}^2(\frac{\sqrt{a}}{2}(kx - \omega t))}{b^2 - ac\left[1 - \tanh(\frac{\sqrt{a}}{2}(kx - \omega t))\right]^2}. \tag{21}
$$

This solution is different from the sec^2-type traveling solitary-wave solution of (1) in [4, 5], but is similar in sense that they possess nonzero backgrounds at infinity.

Figure 1 shows the profiles of the bright and dark solitary-waves in (20), respectively, for different model coefficients α and β by setting, as an example, $\rho_1 = \rho_2 = \rho_3 = 1$, $b = 1$, $c = 1$, and the wave number $k = 1$. It is worth noting that, depending on the signs of the model coefficient the solution becomes a bright solitary-wave for $\alpha\beta > 0$ and a dark solitary-wave for $\alpha\beta < 0$, as shown in Figure 1. The amplitude of the solitary-wave increases with increasing α. However, the nonzero background at infinity of the nonzero solitary-wave solution is unphysical since it can have infinite energy when integrated over x. This can be removed by forcing the nonzero background at infinity to be zero, i. e., $a_0 = 0$, which leads to a special constraints between ρ_1, ρ_2, and ρ_3 for fixed b, c, k, α, and β as

$$
\begin{aligned}
\rho_3 = \frac{1}{2k^2\beta b^2}\big[&-3k^2\beta b^2\rho_2 - 4c \pm (k^4\beta^2 b^4 {\rho_2}^2 \\
&-8k^2\beta b^2\rho_2 c + 16c^2 + 32k^2\beta b^2 c\rho_1)^{1/2}\big].
\end{aligned} \tag{22}
$$

As examples, we plot in Fig. 2 the profiles of the bright and dark solitary-waves, respectively, which have zero backgrounds at infinity. Similar to Fig. 1, we find that the amplitudes of both the bright and dark solitary-waves increase with increasing α. The amplitude of the solitary-wave also increases with decreasing ρ_1 and ρ_2

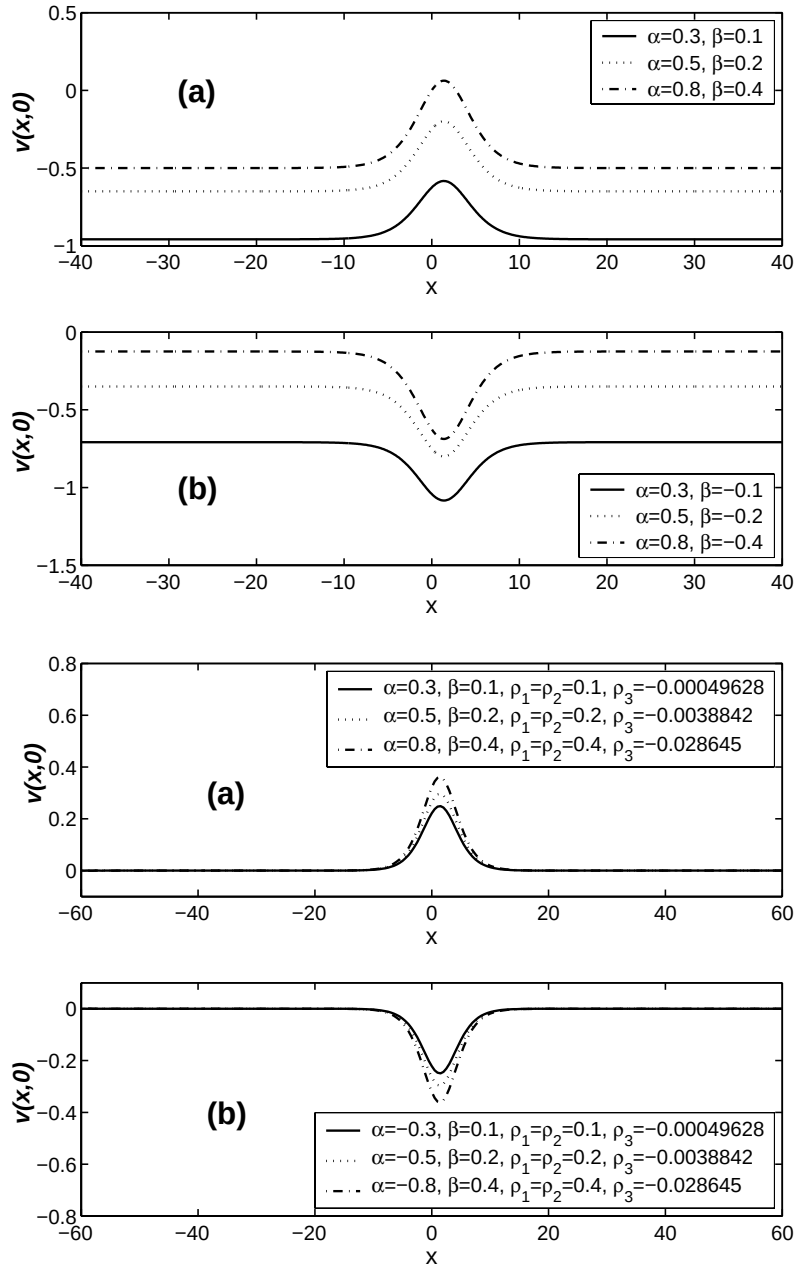

Fig. 1. The profiles of the bright and dark solitary-waves $v(x,0)$ for different model coefficients with the constraint $a = b^2/(4c) > 0$, having a nonzero background at infinity, by setting $\rho_1 = \rho_2 = \rho_3 = 1$, $b = 1$, $c = 1$, and the wave number $k = 1$ for both waves. (a) The amplitude of a bright solitary-wave increases with increasing α. The existence condition for the bright solitary-wave is $\alpha\beta > 0$. (b) The dark solitary-wave exists for $\alpha\beta < 0$ and the amplitude increases with increasing α.

Fig. 2. The profiles of bright and dark solitary-waves $v(x,0)$ for different model coefficients which satisfy the constraint $a = b^2/(4c) > 0$, having zero backgrounds at infinity, by choosing ρ_1, ρ_2, and obtaining ρ_3 from (22). Other parameters for plots are $b = 1$, $c = 1$, and the wave number $k = 1$. (a) The amplitude of the bright solitary-wave increases with increasing α. (b) The amplitude of dark solitary-wave increases with increasing α. Note that the amplitude depends also on ρ_i.

values, as shown in Figure 2. In the rest of this paper, we study the bright and dark solitary-waves' dynamical properties by numerical simulations.

3. Numerical Simulations

In this section, we numerically integrate (1) to understand the stability and dynamics of the solitary-wave solution found in Section 2. Here the definition of "stability" means that the analytic solitary-wave preserves, when it is substituted in (1) and numerically integrated, its initial profile for a long propagation time without losing its energy by radiation. The numerical scheme used in this work is based on the time advance using the Runge-Kutta fourth-order scheme and a pseudo-spectral method using the dis-

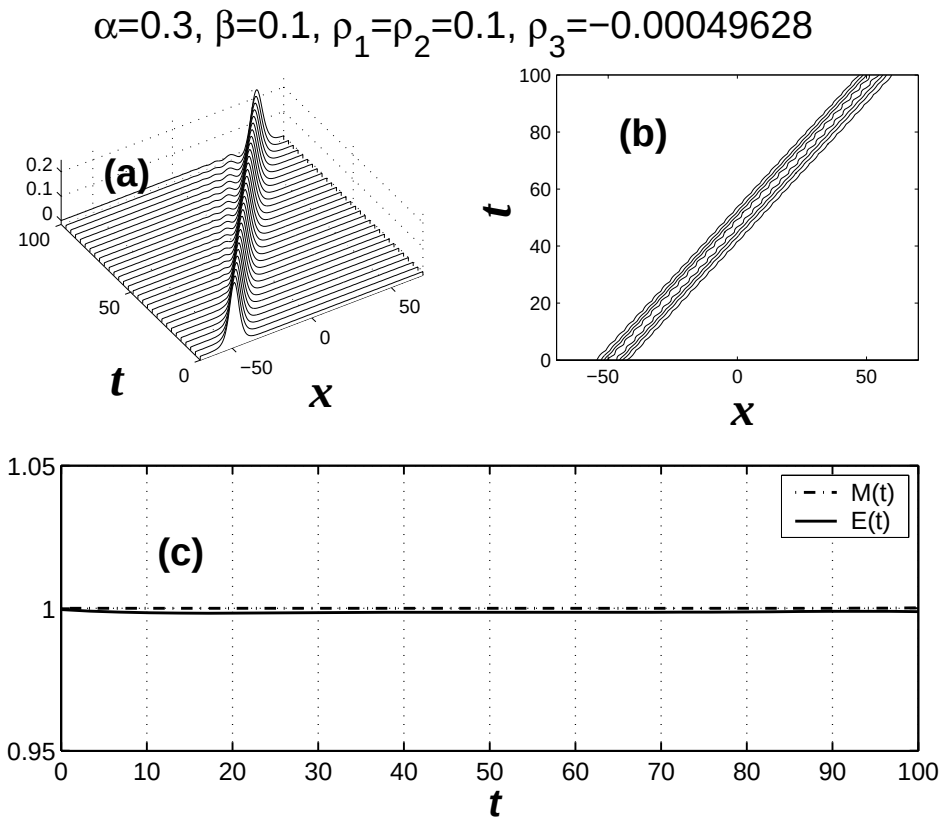

Fig. 3. (a) Evolution of a numerically simulated $v(x,t)$ using the analytic bright solitary-wave as the initial profile. (b) The corresponding contour plot shows a stable solitary-wave propagation up to $t \approx 90$, after which small radiation appears in the form of an oscillating tail. (c) The time evolutions of the normalized mass and energy $M(t)$ and $E(t)$, respectively, which do not deviate from their initial values, indicating the stability of the solitary-wave.

crete fast Fourier transformation in the spatial discretization [13], applying periodic boundary conditions. The numerical errors in the spatial discretization were controlled by varying the number of discrete Fourier modes between 128 to 1024, and various time steps between 10^{-5} to 10^{-3} are chosen for a stable wave propagation.

In the following, we first investigate the stability of the solitary-wave solutions by taking the initial profiles in the form

$$v(x,0)_{\rm init} = -\frac{3k^2\beta b(\rho_3+2\rho_2)}{\alpha\rho_1}\Lambda(x,0) - \frac{6c\beta k^2(\rho_3+2\rho_2)}{\alpha\rho_1}\Lambda(x,0)^2 \quad (23)$$

with the constraint equation (22). Before proceeding, we note that (1) is in general a nonintegrable equation, because it is not certain whether the equation is satisfied by an infinity of time-independent integrals of motion. However, as at least the fundamental solitary-wave solution indeed exists, we define the simplest two such integrals, namely the normalized mass and energy as

$$M(t) = \int_{-\infty}^{\infty} v(x,t)\mathrm{d}x \Big/ \int_{-\infty}^{\infty} v(x,0)\mathrm{d}x \quad (24)$$

and

$$E(t) = \int_{-\infty}^{\infty} v(x,t)^2\mathrm{d}x \Big/ \int_{-\infty}^{\infty} v(x,0)^2\mathrm{d}x, \quad (25)$$

to further understand the dynamics of the waves.

Figure 3a shows the evolution of a numerically simulated $v(x,t)$ using the analytic bright solitary-wave

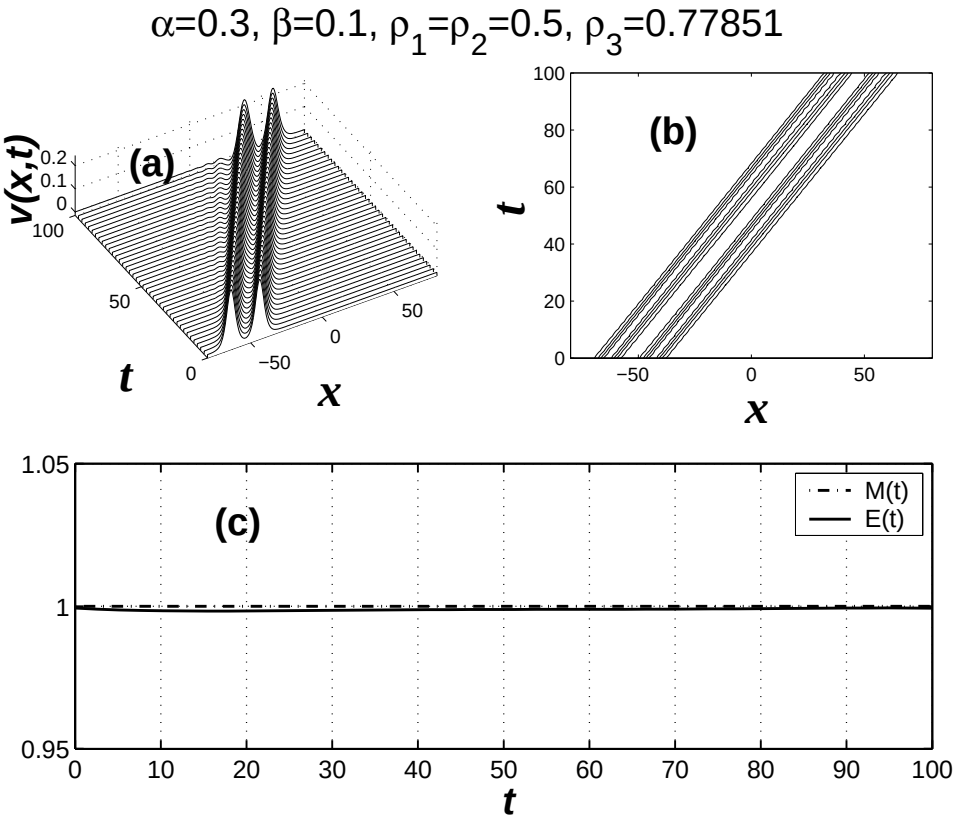

Fig. 4. (a) Interaction dynamics of two bright solitary-waves with the initial profile $v(x+\eta)+v(x-\eta)$, where $\eta = 10$, under the same coefficients α and β as in Fig. 3 but with larger ρ_i values. (b) The stability of the two solitary-waves is maintained according to the contour plot. (c) The stability is accurately confirmed by the conservations of $M(t)$ and $E(t)$.

in (23) as the initial profile. The corresponding contour plot in Fig. 3b demonstrates the stability of the solitary-wave propagation up to $t \approx 90$ after which small radiation appears in the oscillating tail. As shown in Fig. 3c, the time evolutions of the normalized mass and energy $M(t)$ and $E(t)$, respectively, do not deviate from their initial values, which indicates the stability of the solitary-wave. The heuristic reason for this stability is that the highest nonlinear dispersion term (the last term) in (1) is negligible due to the smallness of ρ_3 according to the constraint equation for the zero background at infinity in (22). As a result, the highest nonlinear term, i. e. $\alpha^2\rho_1 v^2 v_x$, balances with the highest nonlinear dispersion term, i. e. $\alpha\beta\rho_2 v v_{xxx}$. A more detailed analysis of the stability of the sech^2-type solitary-wave has been performed by Tzirtzilakis et al. [4, 5]. Even though the evolution of the solitary-wave in Fig. 3 is plotted up to $t = 100$ for a clear picture drawing, the stability of the wave has been maintained for a long propagation time, as demonstrated by the following calculations.

In order to further elaborate the stability of the bright solitary-wave, we consider the evolution of two waves with the initial profile

$$v(x,0)_{\rm inter} = v(x+\eta,0)_{\rm init} + v(x-\eta,0)_{\rm init}, \quad (26)$$

where η is the separation between them. Figure 4a shows the propagation of two bright solitary-waves with the same initial amplitudes, separated by $\eta = 10$, which has been chosen so that the separation distance is larger than the full width at half maximum (FWHM) of the wave, and with larger free parameters: for example, $\rho_1 = \rho_2 = 0.5$. As expected from the result of Fig. 3, the stability of the two solitary-waves is also maintained and more clearly demonstrated in the contour plot in Figure 4b. Furthermore, the stability is accurately confirmed by the conservations of $M(t)$ and $E(t)$ as calculated in Figure 4c.

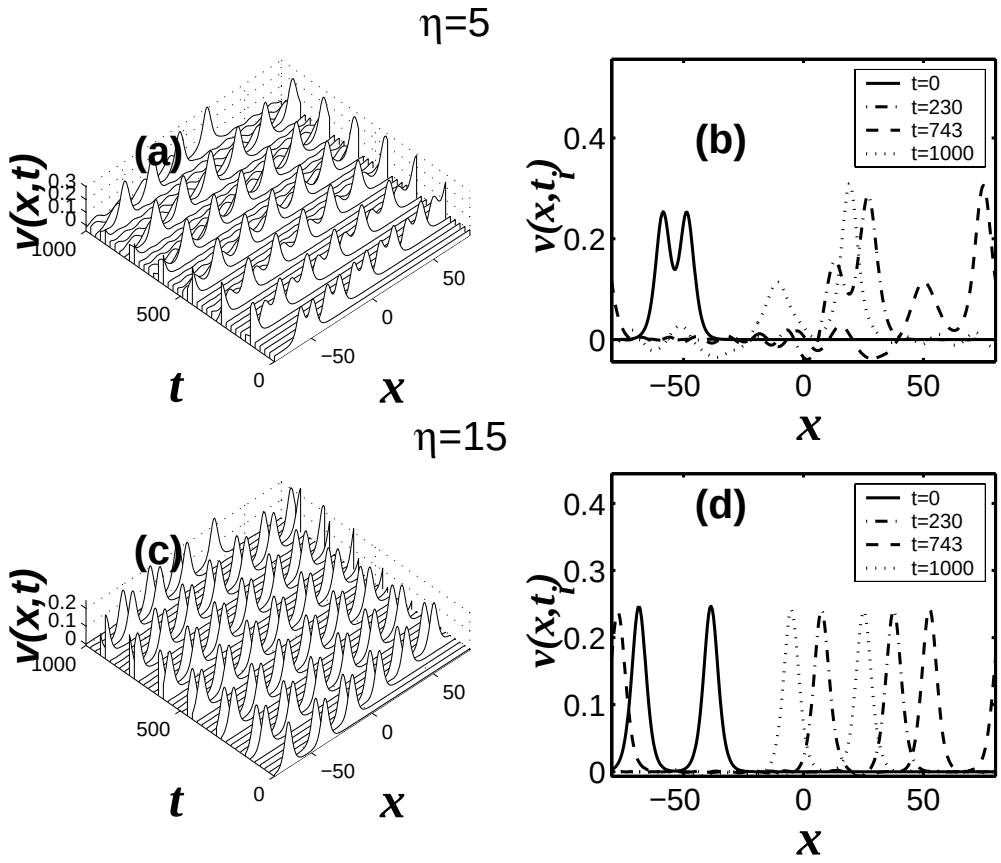

Fig. 5. The same set of model coefficients as in Fig. 4 are used, except η. (a) Evolution of the two bright solitary-waves initially separated by $\eta = 5$, which is smaller than the FWHM of the individual solitary-wave. They propagate as a combined wave but subsequently split into the higher and the lower amplitude waves. (b) Snapshots of the wave profile at different times. As time progresses, the distance between the waves increases while the oscillatory radiation in the tail decreases. (c) The same case as (a) but $\eta = 15$. The two initially separated solitary-waves propagate without mutual interaction. (d) Snapshots of the wave profile show that the initial separation distance is maintained. In comparison with (a), the radiation is completely suppressed.

In Fig. 5 we simulate the evolutions of two solitary-waves with the same initial amplitudes but different separation distances, for example $\eta = 5$ and $\eta = 15$, in order to investigate the effect of η on the evolution when it is taken larger or smaller than the "size" of the individual solitary-waves. For all calculations we have used the same set of model coefficients as in Figure 4. Figure 5a shows the evolution of the two bright solitary-waves separated by $\eta = 5$, which is smaller than the FWHM of the individual solitary-waves: They initially propagate as a combined wave but subsequently split into the higher and lower amplitude waves. The more detailed snapshots of the wave profiles at different times in Fig. 5b indicate that, as time progresses, the distance between the higher and lower waves increases while the oscillatory radiation in the tail decreases. For the case of $\eta = 15$, at which the two solitary-waves are initially separated, the two waves propagate without having any mutual interaction and maintain their stabilities for long evolution times up to $t = 1000$. According to the snapshots of the wave profiles in Fig. 5d, the initial η is maintained during the propagation time. In comparison with Fig. 5a, the radiation in the form of an oscillatory tail is completely suppressed.

We now consider the interaction of two bright solitary-waves with two different amplitudes by taking the initial profile as $v(x,0)_{\rm inter} = 2v(x+\eta,0)_{\rm init} + v(x-\eta,0)_{\rm init}$. Figure 6 simulates the evolution and interaction of the waves. The velocity of the higher

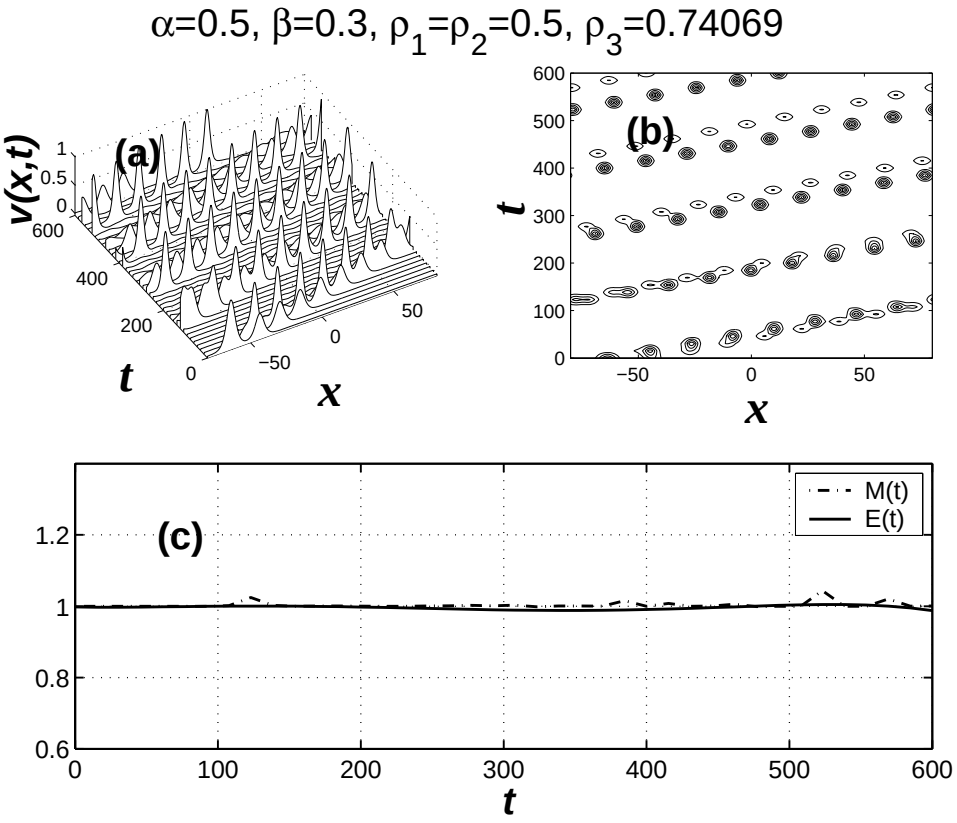

Fig. 6. (a) Interaction dynamics of two bright solitary-waves with two different amplitudes by taking the initial profile as $v(x,0)_{\rm inter} = 2v(x+\eta,0)_{\rm init} + v(x-\eta,0)_{\rm init}$. The higher amplitude solitary-wave catches up the lower one and interacts from left to right, starting at $t \approx 80$ and ending at $t \approx 150$. (b) The contour plot shows a clear separation of the two solitary-waves after the interaction time. (c) The interaction is 'totally elastic' due to the conservation of $M(t)$ and $E(t)$. Sudden increases in the plot are due to the periodic boundary effect.

amplitude solitary-wave is faster than the lower one. As consequence, the higher amplitude solitary-wave catches up the lower one and interacts from left to right starting at $t \approx 80$ and ending at $t \approx 150$, as shown in Fig. 6a, after which the two solitary-waves separate from each other and independently propagate as shown in Fig. 6b. We find in Fig. 6c that the interaction is 'totally elastic' in the sense that the mass and energy of the system conserve their initial values during the time evolution (sudden increases in the plot are due to the periodic boundary effect).

The effects of β, when α and the free parameters ρ_i are fixed, to the dynamics of the two bright solitary-waves with the same profile as in Fig. 6 are shown in Figure 7. Firstly, we notice that as β decreases, as plotted in Figs. 7a – d, the interaction time, as the higher amplitude solitary-wave combines with the lower one, shown in Fig.7, delays. Secondly, we find that the amplitudes of the solitary-waves decrease as β decreases. As the result, the solitary-waves move more slowly and delay the interaction time. Similar to Fig. 6, for all processes in Fig. 7a – d, $M(t)$ and $E(t)$ are accurately conserved. For completeness, we plot the interaction time versus β in Figure 8. The circles represent the interaction times as shown in Figs. 7a – d, respectively, and the solid line is the fitted curve. The stronger β delays the interaction time.

Finally, as an example, we present the simulation result of the two dark solitary-waves with the same initial amplitude separated by $\eta = 10$ in Figure 9. As expected from the above results, the dark solitary-waves show exactly the same dynamical behavior as the bright solitary-waves, since the signs of α and β do not influence on the wave's amplitude except the polarity of the solitary-wave.

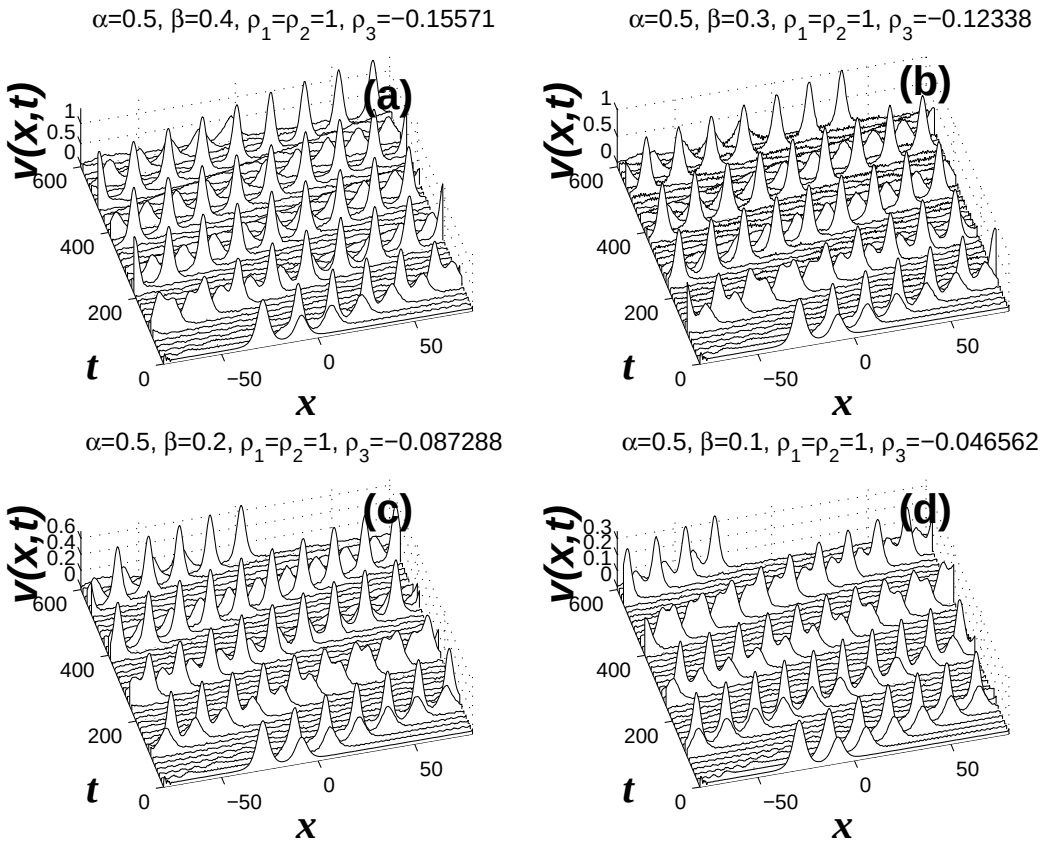

Fig. 7. The effects of β, when α and the free parameters ρ_i are fixed, on the dynamics of the two bright solitary-waves with the same profile as in Figure 6. From (a) – (d) the interaction time, defined as the higher amplitude solitary-wave passes by the lower one, delays. The amplitudes of the solitary-waves decrease as β decreases. For all processes in (a) – (d), $M(t)$ and $E(t)$ are accurately conserved.

4. Conclusions

In this work, we have found the new analytic solitary-wave solution (20) of the higher order KdV equation [1 – 5] by utilizing the auxiliary equation method [10, 11]. The solitary-wave solution (20) exists under $a > 0$ and $b^2 - 4ac = 0$, or $a = b^2/(4c) > 0$. However, the solitary-wave solution possesses a nonzero background at infinity, which is unphysical, since it can have infinite energy when integrated over x, which has been removed by the constraint (22) equation on ρ_1, ρ_2, and ρ_3. The solution processes bright and dark solitary-waves with zero background at infinity, depending on $\alpha\beta > 0$ and $\alpha\beta < 0$, respectively, as shown in Figure 2.

We have investigated by numerical simulations the dynamics of the bright solitary-wave by taking the exact solution in (20) as the initial profile for time propagation. The stable propagation of the bright solitary-wave has been confirmed by investigating the wave's evolution profile and by the conservation of the two physical parameters $M(t)$ and $E(t)$ in Figure 4. The interaction dynamics of two bright solitary-waves has been shown in Figs. 4 – 7. When two solitary-waves are separated by $\eta = 10$ or $\eta = 15$, no mutual interaction has been observed. However, from the simulations of two solitary-waves with different initial amplitudes, we have concluded that the interaction process occurs elastically due to the conservation of the mass and energy. Even though the multi-solitons solution of (1) has not been found yet by current analytical methods, our numerical results may shed light on the existence of such a solution.

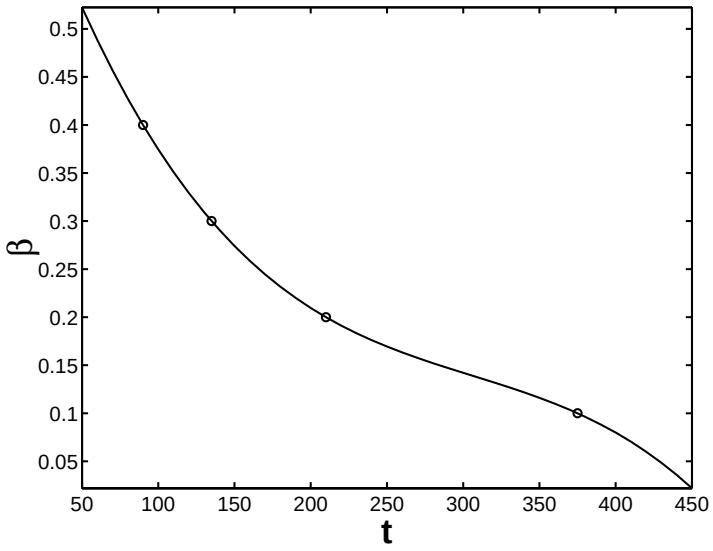

Fig. 8. The interaction time t, defined by the higher amplitude solitary-wave combining with the lower one as shown in Fig. 7, versus the third-order dispersion coefficient β. The circles represent the interaction times as shown in Figs. 7a – d, and the solid line is the fitted curve. The stronger β shortens the interaction time.

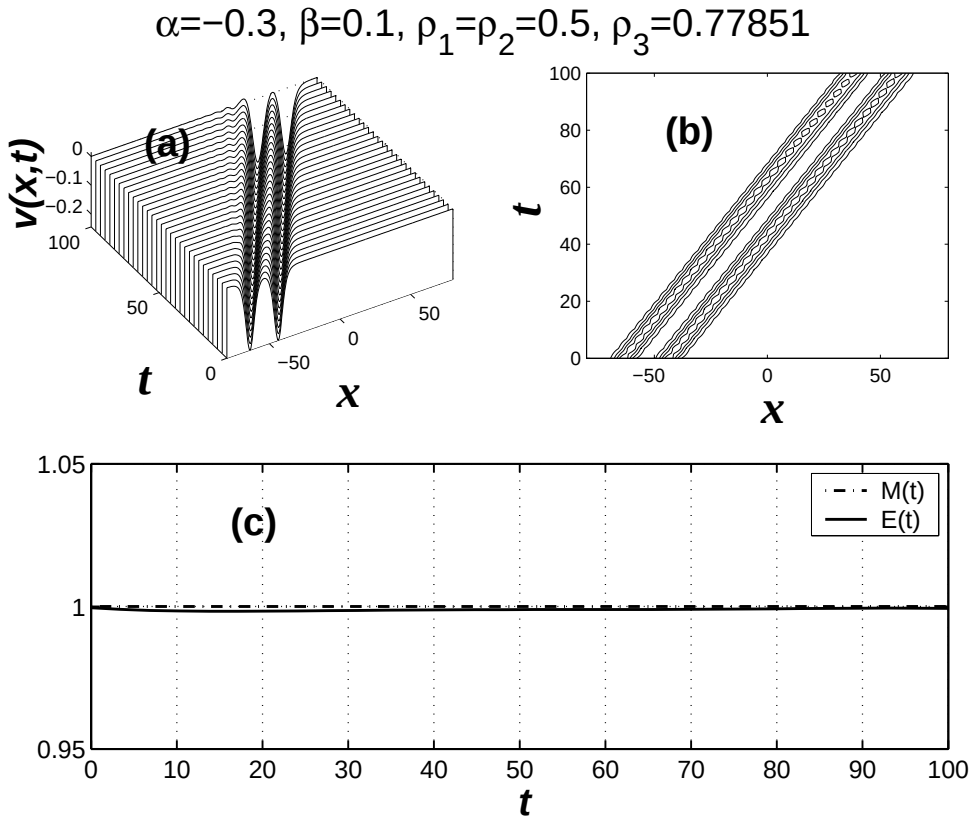

Fig. 9. The same as Fig. 4 except $\alpha < 0$. (a) Interaction dynamics of the two bright solitary-waves with the initial profile $v(x+\eta) + v(x-\eta)$, where $\eta = 10$. It shows at stable propagation. (b) The stability of the two dark solitary-waves is maintained according to the contour plot. (c) The stability is accurately confirmed by the conservations of $M(t)$ and $E(t)$.

Acknowledgement

In 2005 this research was supported by the Catholic University of Daegu. The author thanks the anonymous referee for very detailed comments and suggestion for the improvement of the paper.

[1] S. A. Khuri, Chaos, Solitons and Fractals **26**, 25 (2005).
[2] D. Zwinllinger, Handbook of Differential Equations, Academic Press, London 1989.
[3] M. Ablowitz, P. A. Clarkson, and N. J. Hitchin, Solitons, Nonlinear Evolution Equations and Inverse Scattering, Cambridge University Press, Cambridge 1991.
[4] E. Tzirtzilakis, V. Marinakis, C. Apokis, and T. Bountis, J. Math. Phys. **43**, 6151 (2002).
[5] E. Tzirtzilakis, M. Xenos, V. Marinakis, and T. Bountis, Chaos, Solitons and Fractals **95**, 87 (2002).
[6] Y. Long, Y. Rui, and B. He, Chaos, Solitons and Fractals **23**, 469 (2005).
[7] J. Li and Z. Liu, Appl. Math. Model **25**, 41 (2000).
[8] J. Li and Z. Liu, Chin. Ann. Math. **23B**, 397 (2000).
[9] A. Jeffrey and M. Mohamad, Chaos, Solitons and Fractals **2**, 187 (1991).
[10] E. V. Krishnan, J. Math. Phys. **31**, 1155 (1990).
[11] E. Yomba, Chaos, Solitons and Fractals **21**, 75 (2004).
[12] J. J. Kim and W.-P. Hong, Z. Naturforsch. **59a**, 721 (2004).
[13] L. N. Trefethen, Spectral Method in Matlab, Society for Industrial and Applied Mathematics, Philadelphia 2000.